Stratigraphic context for reef-building microbialites in the Tonian Reefal assemblage (Fifteenmile Group) of the Yukon

*Charlotte Spruzen**
McGill University

Katie M. Maloney
Royal Ontario Museum

J. Wilder Greenman
Dalhousie University

Maxwell A. Lechte
University of Melbourne

Galen P. Halverson
McGill University

Spruzen, C., Maloney, K.M., Greenman W.J., Lechte, M.A. and Halverson, G.P., 2025. Stratigraphic context for reef-building microbialites in the Tonian Reefal assemblage (Fifteenmile Group) of the Yukon. *In*: Yukon Exploration and Geology Technical Papers 2024, L.H. Weston, A. Stuart, S.K. Schultz, A.D. Brubacher and D.C. Cronmiller (eds.), Yukon Geological Survey, p. 75–95.

Abstract

The Tonian Period (1000–720 Ma) likely represents a critical transition in microbial reef construction, given the emergence of reefs built by thrombolites and other cavity-dense microbialites. However, there are few detailed studies on Tonian reef development to constrain this ecologically significant transformation. Here, we build on previous documentation of reefal buildups in the ca. 850–780 Ma Fifteenmile Group in the Coal Creek inlier (Ogilvie Mountains) and contribute seven new detailed stratigraphic sections featuring microbial accumulations in the Reefal assemblage. We document the stratigraphic context for these Tonian reefs and distinguish between predominantly laminated and unlaminated microbial textures. In addition, we identify rare instances of exceptional preservation of unlaminated microbialite, suggesting that reef-building microbialites of the Reefal assemblage have similar framework morphologies to those of the approximately coeval Little Dal Group in the Mackenzie Mountains.

Plain language summary

Before the evolution of animals, reefs were formed of carbonate rock built by micro-organisms. It has been suggested that around one billion years ago, these microbial reefs went through a transition from simple layered structures to complex clotted, three-dimensional frameworks. To better understand this transition, we studied an 800 to 850 million-year-old reef exposed in the Ogilvie Mountains of the Yukon, on the Traditional Territory of the Tr'ondëk Hwëch'in First Nation. We document substantial reefs that built up on uplifted topography, adjacent to a deeper-water basin of shale and carbonate rocks. We also demonstrate for the first time that these reefs were built by clotted frameworks, with strong similarities to reefs of the same age from the Northwest Territories.

* charlotte.spruzen@mail.mcgill.ca

Introduction

It has been suggested that the Tonian Period represents a pivotal point in reef evolution, during which thrombolites and cavity-dense microbialite frameworks became volumetrically important reef-builders for the first time (Grotzinger and James, 2000; James and Jones, 2015). This hypothesis was largely based on observations from the Tonian Little Dal Group of the Mackenzie Mountains (Northwest Territories; Fig. 1), specifically the Stone Knife and Silverberry formations, which contain reefs built by a consortium of shallow-water stromatolites (Batten et al., 2004) and deep-water calcimicrobes (Turner et al., 1993, 1997, 2000). The Fifteenmile Group is thought to correlate with the Little Dal Group based on lithostratigraphic and chemostratigraphic correlations integrated with available geochronological constraints (Macdonald et al., 2012; Thomson et al., 2015a, b). Therefore, further investigation into the timing of reef development and the nature of reef-building organisms in the Reefal assemblage could aid in correlating Tonian strata across northwestern Canada and provide additional insight into the evolution of Neoproterozoic reef complexity.

The Reefal assemblage is a mixed carbonate-siliciclastic formation within the Tonian Fifteenmile Group in the Coal Creek and Tatonduk inliers of central western Yukon (Fig. 1 ; Macdonald et al., 2010b, 2012; Halverson et al., 2012). This formation is considered to record platformal reef development on the footwall of normal faults and successive shale-to-carbonate transitions in the adjacent basin, reflecting transgressive-regressive sequences (Macdonald et al., 2012). The shales and slope carbonates of the Reefal assemblage have been the subject of detailed studies, including investigations of carbonate carbon isotope ($\delta^{13}C_{carb}$) variability and the onset of the global Bitter Springs negative carbon isotope anomaly (Coal Creek inlier; Macdonald et al., 2010a), as well as paleoredox geochemistry of black shales (Coal Creek inlier; Sperling et al., 2013 ; Gibson et al., 2020) and apatitic scale microfossils (age-equivalent assemblage in the Tatonduk inlier; Cohen et al., 2017).

In this report, we present stratigraphic sections of the Fifteenmile Group from the Coal Creek inlier, with a focus on the Reefal assemblage (Fig. 2). Previous authors have described the Proterozoic geology of the inlier (Green, 1972; Thompson and Roots, 1982; Thompson et al., 1994; Strauss et al., 2014) and the basin-scale reef stratigraphy of the Reefal assemblage (Macdonald and Roots, 2010; Macdonald et al., 2010b, 2012; Halverson et al., 2012). In this study we focus on documenting microbialite facies within their stratigraphic context. We observe a substantial prograding platformal reef system that is largely composed of framework-constructing microbialites.

Geological history

The Yukon block is a crustal promontory on the northwest corner of Laurentia, bound to the east by the Richardson fault array and to the south by the Dawson thrust fault (Fig. 1a). Neoproterozoic strata of the Yukon block are exposed in a series of inliers and broadly correlate across them, as well as with thick Neoproterozoic successions in the Mackenzie Mountains to the east, and the Amundsen basin (including the Minto Inlier and the Brock Inlier) to the northeast (Rainbird et al., 1996; Thomson et al., 2015a, b; Greenman et al., 2020). These strata were originally divided into three sequences (A, B and C) based on major unconformities that can be correlated across the region (Young et al., 1979). In the Coal Creek inlier, these strata range in age from the polydeformed siliciclastic-carbonate succession of the ca. 1600 Ma Wernecke Supergroup (sequence A; Young et al., 1979; Thorkelson et al., 2005; Furlanetto et al., 2013) to the Ediacaran Rackla Group of sequence C (Busch et al., 2021).

Sequence B (ca. 1.2–0.8 Ga) begins with the Pinguicula Group, a siliciclastic-carbonate succession that unconformably overlies the Wernecke Supergroup and the Hart River sills (Medig et al., 2016). The age of the Pinguicula Group has recently been hypothesized to be ca. 1.1 Ga based on correlation with the Amundsen and Bylot basins (Greenman et al., 2021). In the Ogilvie Mountains, the Pinguicula Group is unconformably overlain by the Fifteenmile Group, which was originally divided into 'upper' and 'lower' subgroups with five and three map units, respectively (Thompson et al., 1994). More recently, four distinct formations were defined within the Fifteenmile Group in the Coal Creek inlier (Halverson et al., 2012; Kunzmann et al., 2014), which together record a series of coherent transgressive-regressive cycles without major unconformities. The informal Gibben formation is characterized by a shallowing-up succession that progresses from wavy laminated dolomudstone containing common molar-tooth structure, to shallow marine oolitic grainstones and tidal flat, microbially laminated carbonates (Macdonald et al., 2012; Kunzmann et al., 2014). The upper subaerial exposure surface of the Gibben formation is conformably overlain by deltaic facies of the formalized Chandindu Formation (Kunzmann et al., 2014), comprising predominantly maroon to green-weathering siltstone including shale to siltstone to

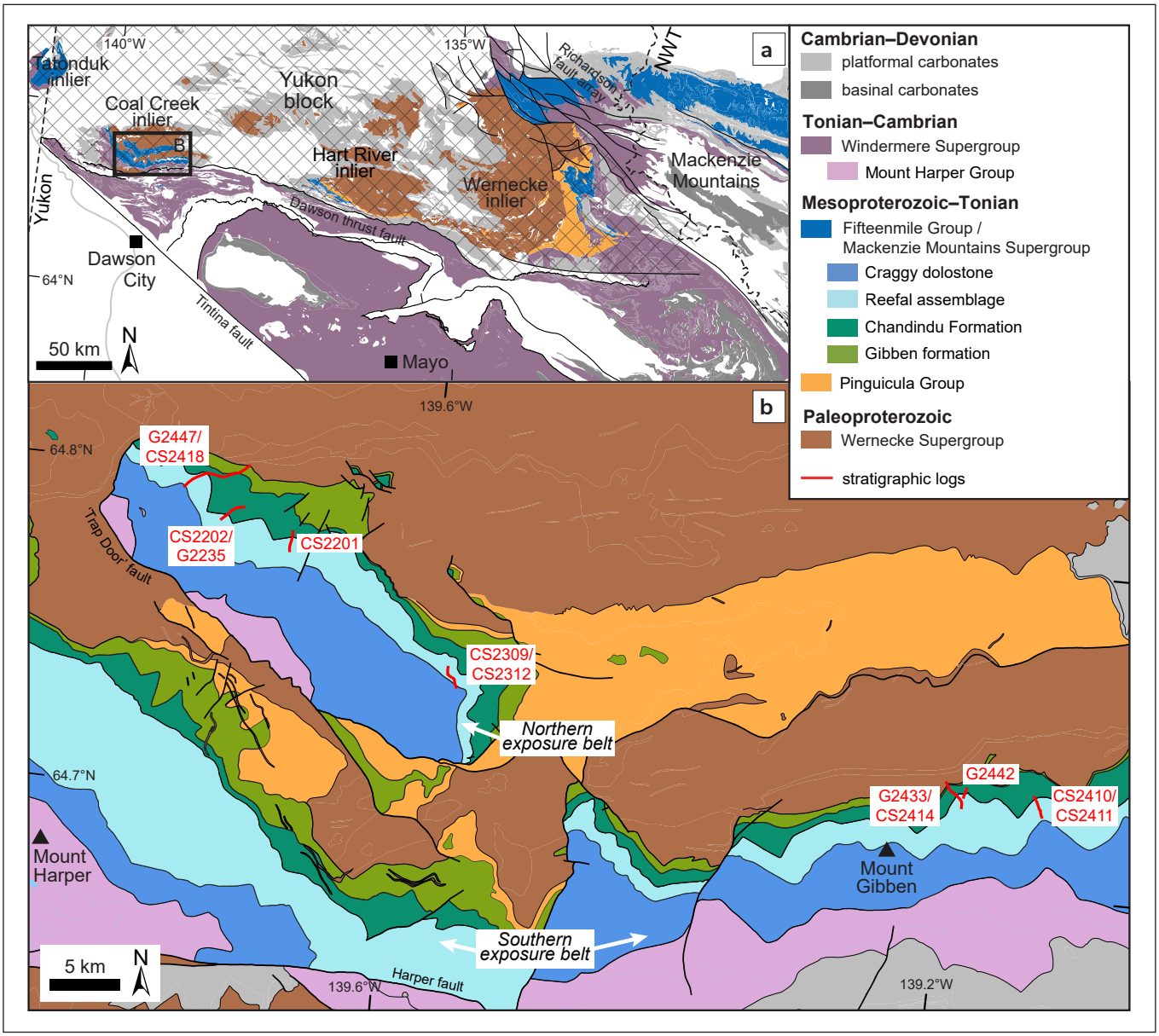

Figure 1. *Geology of the study area:* ***(a)*** *Simplified geological map of Proterozoic strata in the Yukon and Northwest Territories (after Colpron et al., 2016), delineating the location of the study area (Coal Creek inlier) relative to other Proterozoic inliers.* ***(b)*** *Inset of (a); geological map of the Coal Creek inlier (after Strauss et al., 2014). Legend is the same as (a), except for the Fifteenmile Group, which is separated into its four constituent formations. Stratigraphic sections measured as part of this study are denoted in red. The study area has been annotated to show two belts of exposure separated by the 'Trap Door' fault (Strauss et al., 2015).*

dolostone cycles, as well as horizons of stromatolitic dolostone and channelized sandstone (Macdonald et al., 2012; Kunzmann et al., 2014). An abrupt contact characterized by a dark, organic-rich shale, and most pronounced in proximal settings, marks a major flooding surface and separates the Chandindu Formation from the Reefal assemblage (Macdonald et al., 2012). The abrupt re-establishment of marine conditions is followed by the development of a platformal reef system (Halverson et al., 2012; Macdonald et al., 2012), which is the topic of this contribution. The upper contact of the Reefal assemblage is a subaerial exposure surface, which is overlain by the heavily recrystallized and silicified grainstones and debrites of the Craggy dolostone, interpreted to record progradation of a thick, laterally extensive carbonate platform (Halverson et al., 2012; Macdonald et al., 2012).

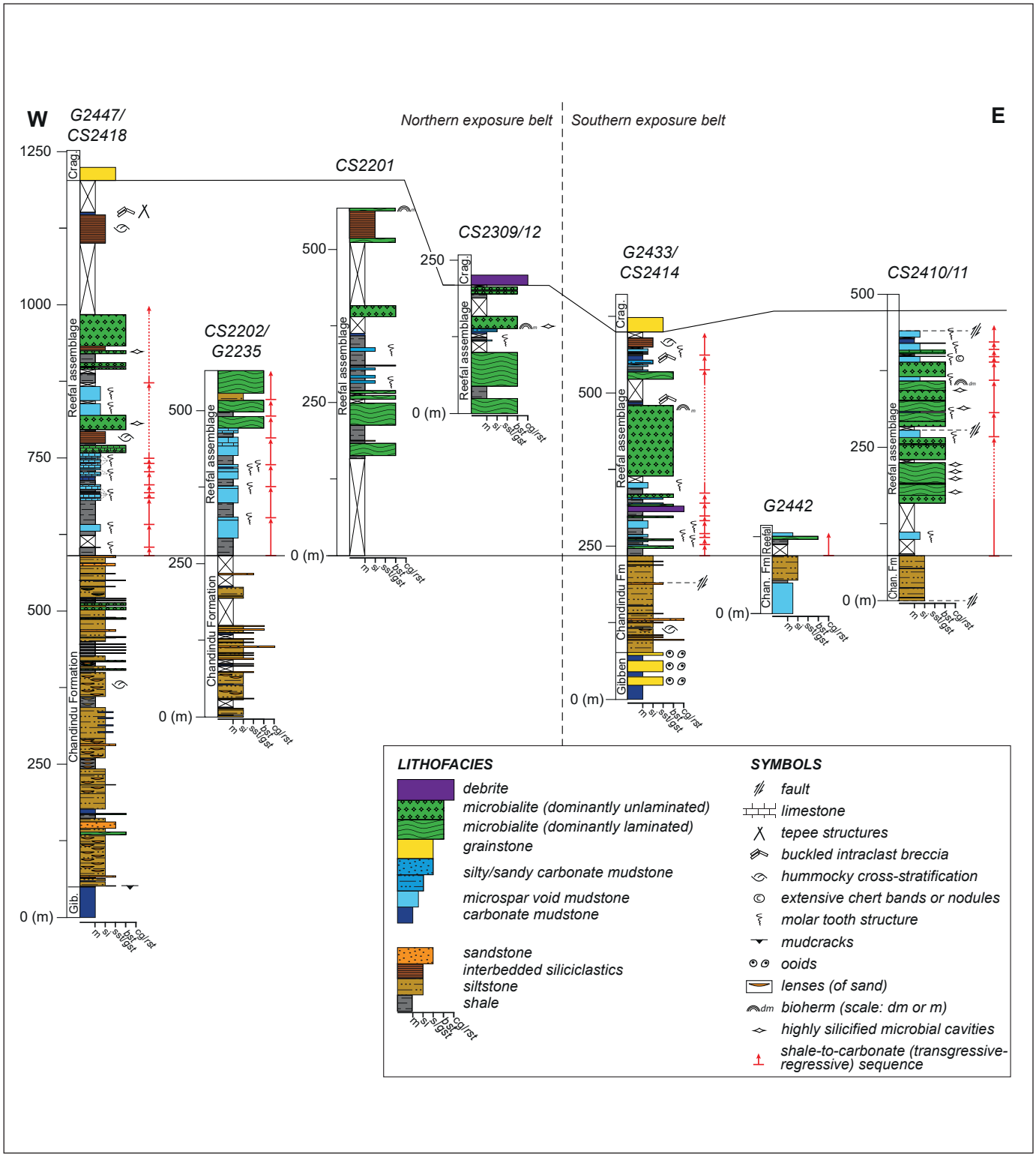

Figure 2. *Logs of stratigraphic sections measured through the Fifteenmile Group. Section locations are denoted in Figure 1b, and their coordinates are listed in Table 2. The x-axes refer to increasing grain size of siliciclastic rocks (m: mudstone, si: siltstone, sst: sandstone, cg: conglomerate) and Dunham classification of carbonates (m-si: mudstone, gst: grainstone, rst: rudstone). The y-axis refers to stratigraphic height (perpendicular to regional bedding) in metres, levelled to the Chandindu Formation–Reefal assemblage contact. Gib.: Gibben formation, Chan.: Chandindu Formation, Crag.: Craggy dolostone, Fm: Formation.*

The Fifteenmile Group exhibits significant lateral variation in both facies and thickness of individual units, and much of this discrepancy is attributed to its deposition during a period of active extension and related growth faulting (Macdonald et al., 2012). The Gibben formation has the highest lateral variability in thickness due to its deposition during a phase of syndepositional normal faulting, which developed a horst and graben basin bathymetry (Macdonald et al., 2012). Variations in thickness and lithology continue in the overlying Chandindu Formation due to its deposition on this rift-inherited complex basin topography, as well as continued syndepositional faulting (Macdonald et al., 2012; Kunzmann et al., 2014). Coarsening-upward cycles from shale to sandstone to carbonate are common throughout the Chandindu Formation, but the carbonate facies vary significantly and range from supratidal to below storm-wave base, indicating that carbonate deposition was ongoing, accumulating locally during lapses in siliciclastic input (Kunzmann et al., 2014).

A flooding surface, marked by deposition of deeper-water, organic-rich shale, forms the base of the Reefal assemblage and is ubiquitous across the basin. Higher in the succession, the Reefal assemblage also demonstrates significant lateral variability (Macdonald et al., 2012). Though this was variably attributed to thrust repetition (Thompson et al., 1994), the conformable nature of stratigraphic contacts prompted a reinterpretation of the formation as a platformal reef system with coeval shale and carbonate deposition (Halverson et al., 2012; Macdonald et al., 2012). On inferred paleotopographic highs on the uplifted footwall of north-northwest-side-down normal faults, the Reefal assemblage consists predominantly of platformal microbialite buildups (Macdonald et al., 2012). In the basinal settings of the hanging wall, the Reefal assemblage comprises shale-to-carbonate cycles, and the predominant carbonate facies is laminated carbonate mudstone containing extensive molar-tooth structure and internal brecciation (Macdonald et al., 2012). These cycles are interpreted as transgressive-regressive sequences where highstand systems tracts correspond to progradation of the platform reefal buildups (Macdonald et al., 2012). Mass-flow deposits and olistoliths also occur in these slope-to-basinal settings (Macdonald et al., 2012).

Two radiometric ages have been obtained on the Reefal assemblage: a U-Pb zircon age of 811.51 ± 0.25 Ma from a tuff in basinal facies near the top of the Reefal assemblage in the Coal Creek inlier (Macdonald et al., 2010a), and a statistically overlapping Re-Os age of 810.7 ± 6.3 Ma from just below a fossiliferous horizon of the correlative Upper Tindir Group in the Tatonduk inlier (Cohen et al., 2017). The base of the Reefal assemblage is poorly constrained, having a maximum depositional age of ca. 1000 Ma based on U-Pb dating of detrital zircon in the Reefal assemblage and the Chandindu Formation (Gibson et al., 2021). The top is directly constrained by a 752.7 ± 5.5 Ma Re-Os age from the base of the Callison Lake Formation (Rooney et al., 2015), but the continuation of the globally correlative Bitter Springs $\delta^{13}C$ anomaly into the lower Craggy dolostone implies a minimum age constraint of ca. 800 Ma (Macdonald et al., 2010a; Halverson et al., 2022). Thus, in the absence of major unconformities within the Reefal assemblage, an age range of ca. 850–800 Ma is inferred (e.g., Gibson et al., 2020).

Lithofacies descriptions

Sections of the Fifteenmile Group were documented using carbonate (Figs. 3–5) and siliciclastic (Fig. 6) lithofacies, described in Table 1. The carbonate lithofacies were based broadly on Dunham's classification scheme, including an internal division in the categories of boundstone and mudstone. Given the lack of observable features in many outcrop faces of the Reefal assemblage, it was impractical to use established terms such as stromatolite (Kalkowsky, 1908) or thrombolite (Aitken, 1967) to describe microbialites, because their defining features in the field—accretionary laminations radiating from a fixed surface (Semikhatov et al., 1979) and clotted mesostructure (Shapiro, 2000), respectively—could only be identified in rare cases. Therefore, we used a bimodal division of microbialites into dominantly laminated and dominantly unlaminated textures (Table 1; Fig. 4) highlighted by cavities (such as fenestrae) composed of either dolomite microspar or silica. The microbialite is locally variable, but facies are classified by the dominant features seen on a metre scale. Carbonate mudstones (calcimudstone and dolomudstones) were divided based on the presence of abundant cements, which we interpret to be pre- or syn-compaction and lithification, such as molar-tooth structure (Table 1).

Section descriptions

Southern exposure belt (east to west)

Section CS2410/11

At the base of the easternmost section, between Mount Gibben and the Chandindu River (64.7294°N, 139.1229°W; Figs. 1b and 2, Table 2), the Chandindu Formation comprises ~75 m of maroon to grey-green

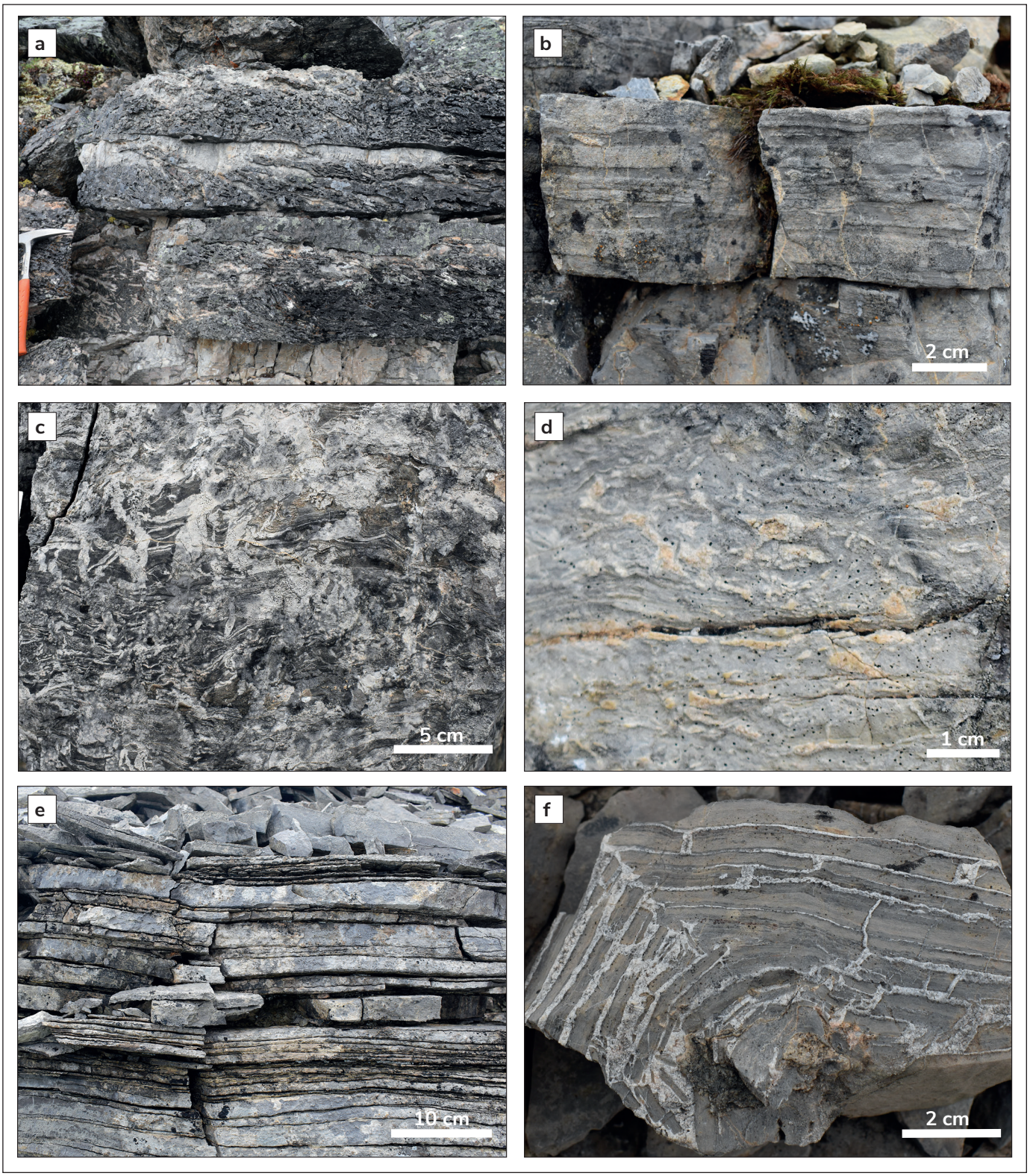

Figure 3. *Field photographs of carbonate facies of the Reefal assemblage, excluding microbialite.* ***(a)*** *Debrite beds with tabular clasts in a heavily silicified matrix. Rock hammer for scale measures ~33 cm.* ***(b)*** *Dolomudstone with thin interbeds of very fine quartz sand.* ***(c)*** *Microspar-void calcimudstone facies, with extensive molar-tooth structure distorting planar laminated dolomudstone.* ***(d)*** *Microspar-void dolomudstone facies, with round, elongate dolomite microspar cement seams.* ***(e)*** *Laminated dolomudstone.* ***(f)*** *Dolomudstone with buckled tabular internal breccia.*

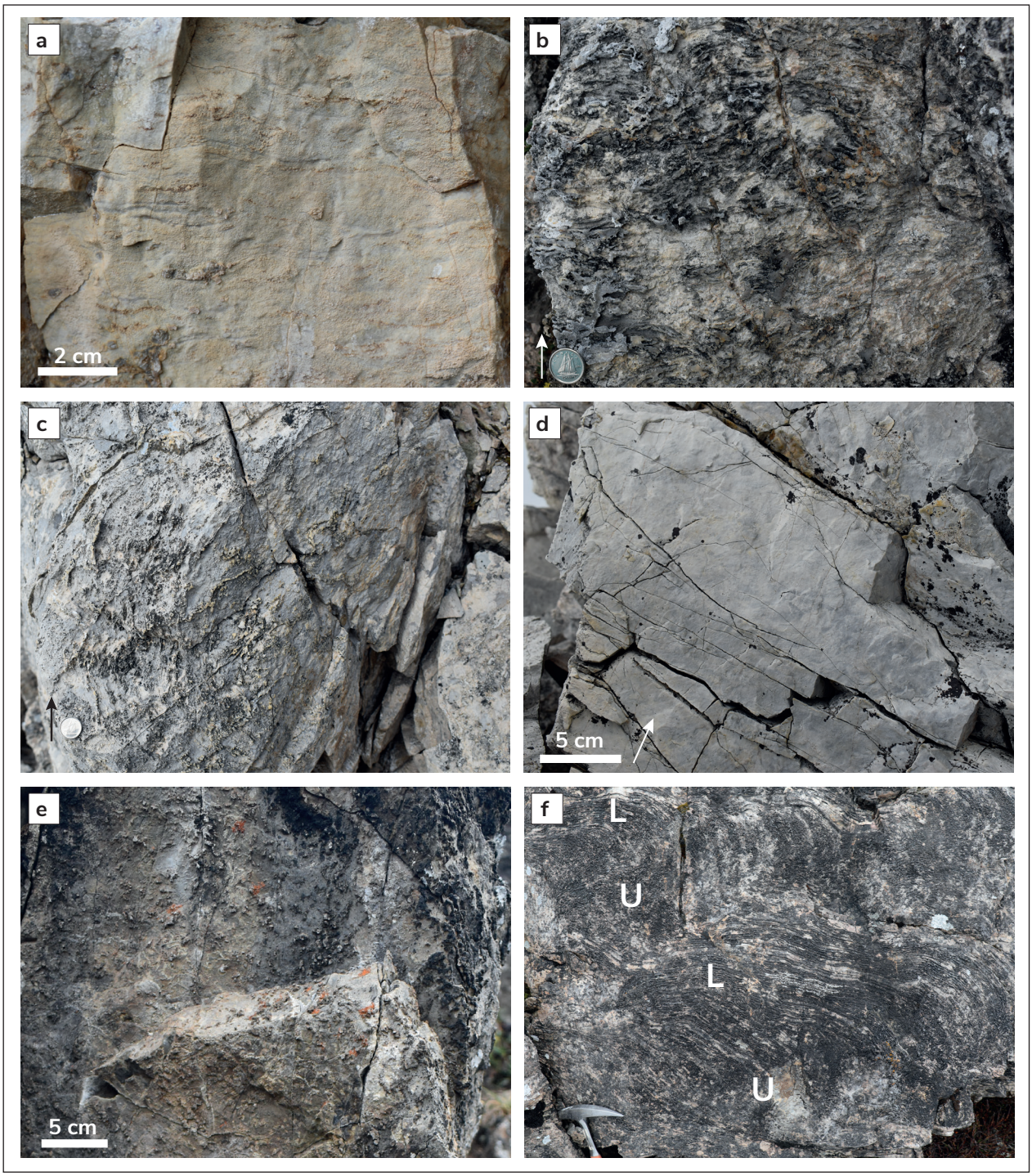

Figure 4. *Field photographs of archetypal microbialite doloboundstone of the Reefal assemblage.* ***(a)*** *Typical example of laminated microbialite doloboundstone, with faint, bedding-parallel laminations of orange-weathering microspar.* ***(b)*** *Extensively silicified microbialite doloboundstone, with prominent elongate, bedding-parallel lenses of crystalline silica (arrow denotes way-up direction). Canadian dime for scale is 1.8 cm in diameter.* ***(c)*** *Domal stromatolite defined by silicified elongate fenestrae, with laminations at a high angle to regional bedding (arrow denotes way-up direction). Canadian dime for scale.* ***(d)*** *Typical example of unlaminated microbialite doloboundstone, preserved as massive dolomite with no discernable features other than a slight mottling between shades of light grey. Arrow denotes way-up direction.* ***(e)*** *Extensively silicified unlaminated microbialite doloboundstone, with prominent, low aspect-ratio protrusions of crystalline silica.* ***(f)*** *Highly silicified microbialite bioherms that transition from unlaminated microbialite at the base and centre (U) to laminated microbialite at the outer edges (L).*

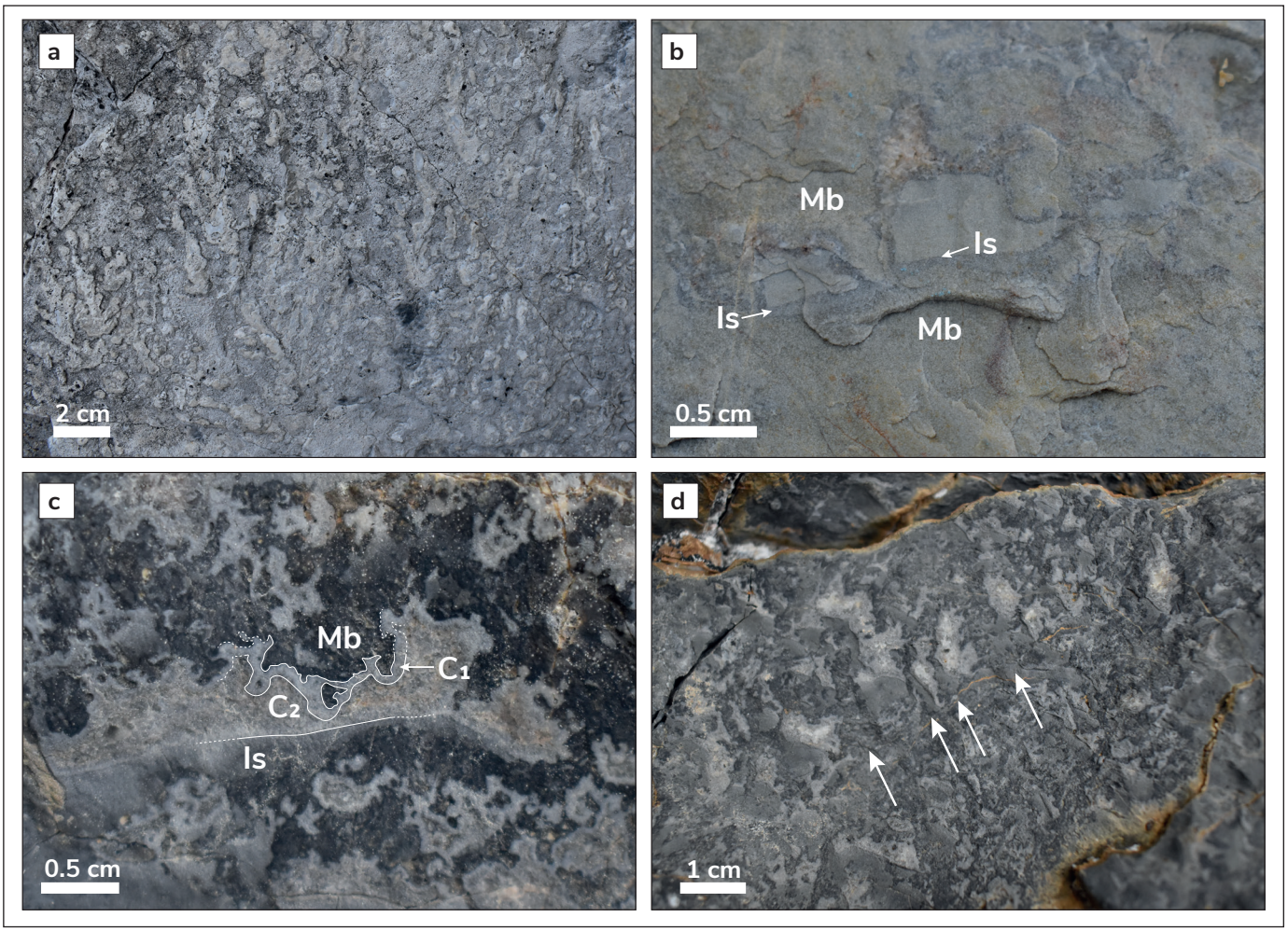

Figure 5. *Field photographs of exceptionally well-preserved microbialite boundstone of the Reefal assemblage.* ***(a)*** *Microbialite doloboundstone from stratigraphic section CS2411, with columnar, locally dendritic texture defined by a sharp distinction between light and dark dolostone, reflecting cavity space and microbialite, respectively.* ***(b)*** *Microbialite doloboundstone from stratigraphic section CS2414, with textural variation between tan-weathering microbialite (Mb) and slightly blue-tinged cavity fill. Note the layer of dark internal sediment (ls) spanning either side of the microbialite bridge bisecting the cavity.* ***(c)*** *Microbialite calciboundstone from stratigraphic section CS2418, displaying a dark, clotted microbial framework (Mb). Cavities are filled with internal sediment (ls) and two generations of cement: the first (C_1) is a <1 mm outline of the upper surface of the microbialite cavity, and the second (C_2) is a tan-weathering later-stage fill.* ***(d)*** *Wider view of the microbialite calciboundstone from stratigraphic section CS2418; arrows show local columnar growth of dark microbialite. Cavities between the columns have internal sediment and later-stage cement, creating geopetal structures.*

weathering siltstone, with rare ~5 cm interbeds of orange, laminated dolomudstone (occurring approximately every ~20 m). The base of the Reefal assemblage is marked by a distinct interval of black shale that is 3 m thick. The lowermost dolostone outcrop is microspar-void dolomudstone, with thin, bedding-parallel microspar seams and small-scale molar-tooth structure throughout. This is overlain by ~65 m of doloboundstone microbialite, which alternates between laminated microbialite with dense, prominent silicified cavities at a high angle to regional bedding; laminated microbialite with faint, elongate microspar cavities at a low angle to regional bedding; and massive microbialite with no cavities. Molar-tooth dolomudstone onlaps the top of the uppermost bed of microbialite.

The section resumes approximately 50 m to the southeast on an adjacent ridge exposure. We infer a fault with limited displacement separating the ridges, as the stratigraphic thickness of the adjacent ridge is approximately the same. The succeeding 75 m consists of a prominent outcrop of primarily microbialite

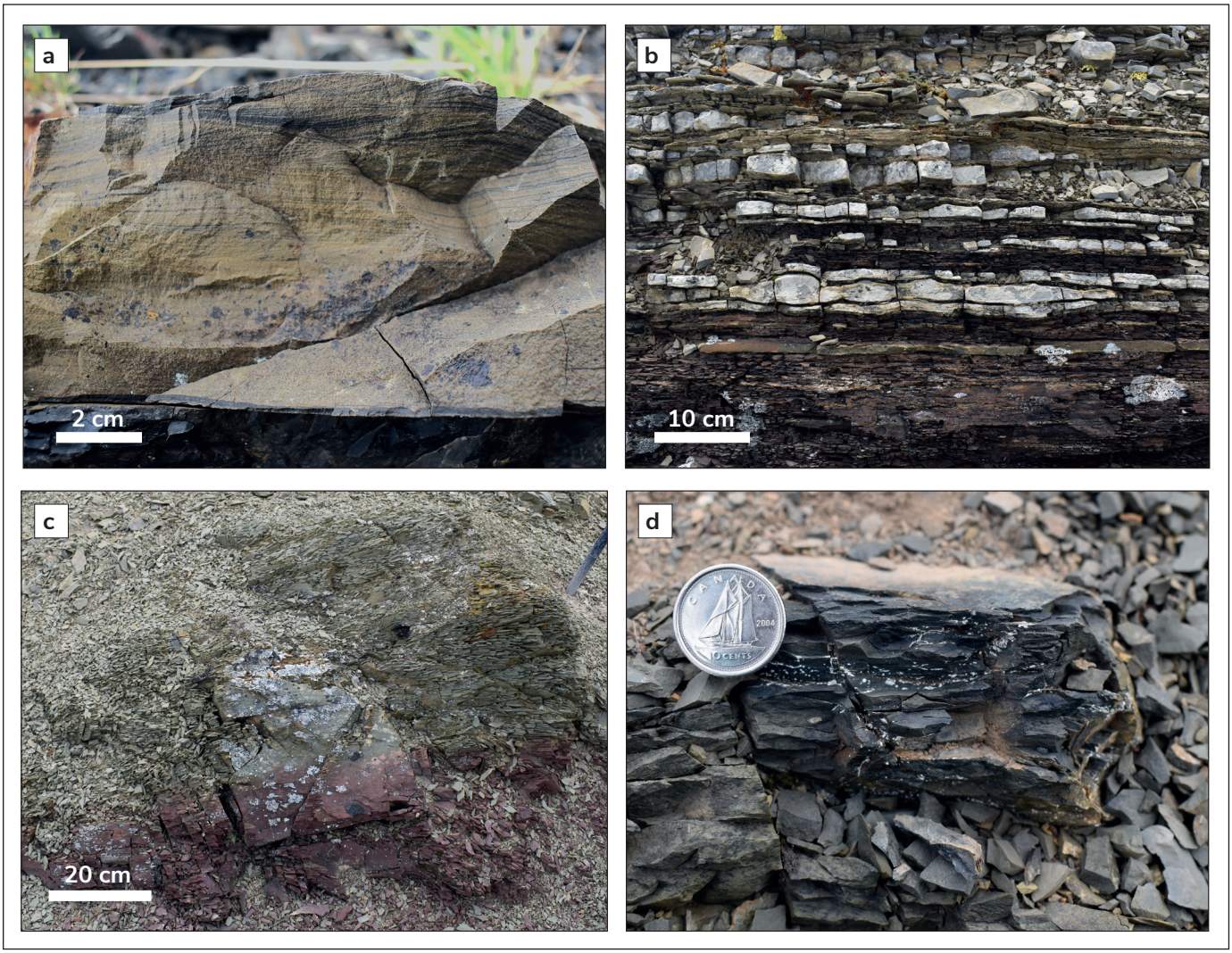

Figure 6. *Field photographs of siliciclastic facies of the Chandindu Formation and the Reefal assemblage.* ***(a)*** *Very fine quartz sandstone, with hummocky cross-stratification at the top of the bed.* ***(b)*** *Interbedded siliciclastic facies, predominantly composed of maroon shale and tan silt, with regular beds of very fine sandstone with calcite cement.* ***(c)*** *Typical outcrop of siltstone, grading from maroon to tan.* ***(d)*** *Typical example of black shale subcrop. Canadian dime, for scale, is 1.8 cm diameter.*

doloboundstone, and internal structure varies between unlaminated, faintly laminated low angle, and highly silicified high angle. Preservation quality is mixed at the outcrop scale, and one face displays a columnar, potentially dendritic texture (Fig. 5a). At the top of the exposure, 0.5 m bioherms are defined by low-angle laminations.

Above this, microspar-void dolomudstone contains abundant molar-tooth structure, chert bands and nodules. The top of the section consists of multiple cycles of microspar-void or parallel-laminated dolomudstone overlying microbialite doloboundstone.

Section G2442

This short section, between CS2410/11 and G2433/CS2414 (64.7305°N, 139.1768°W; Figs. 1b and 2, Table 2), was logged through a 50 m interval of dolostone that is absent from the G2433 ridge (only 200 m to the west). This outcrop comprises crudely medium-bedded, microspar-void dolomudstone, and pockets of darker dolomudstone with molar-tooth cements. Above the dolomudstone, black shale grades upward into grey siltstone, followed by green to maroon siltstone typical of the Chandindu Formation. We place the Chandindu–Reefal contact above the variegated siltstone, at the transition to dark soil interpreted to represent a thick

Table 1. *Lithofacies descriptions for the Reefal assemblage and Chandindu Formation, used for the stratigraphic logs in Figure 2. Gf: Gibben formation, CF: Chandindu Formation, Ra: Reefal assemblage and Cd: Craggy dolostone.*

Lithofacies	Description	Occurrence	Figure
debrite	Gravel to boulder-sized tabular, angular to subangular clasts. Some debrites are clast-supported, others are within a dolomudstone matrix. Clasts are primarily parallel-laminated dolomudstone, although some are extensively silicified.	Ra, Cd	3a
laminated microbialite doloboundstone	White to tan-weathering dolostone with crinkly lamination. Laminae are not laterally continuous and may be faint, marked by fenestrae and sheet cavities filled with microspar, or may be strongly resistant due to extensive silicification. Laminae vary in their orientation, and may be bedding parallel or at a high angle to bedding. There are domal stromatolites of 0.1–1 m radius.	Ra	4a–c
unlaminated microbialite doloboundstone	White to tan-weathering dolostone. Most outcrop faces are massive. Rare outcrop faces show irregular, low aspect-ratio cavities with no lamination or orientation (Figs. 5e and 6), which may be accentuated by silicification. Where well exposed, outcrop faces display columnar and dendritic growth of a microbialite framework, and cavities are (partially) filled by internal sediment.	Ra, CF	4d–f, 5a–d
sandy/silty carbonate mudstone	Interbedded dolomudstone with quartz silt or fine sand. Laminae/beds are 1–5 cm thick. Grey chert nodules are common in the thicker sand layers.	Ra	3b
microspar-void mudstone	Finely laminated calcimudstone or dolomudstone with distortion by voids filled with carbonate microspar cements. Many of these cements are the classic endmember form of molar-tooth structure as sheet-like ribbons with homogenous microspar (Kriscautzky et al., 2022). Others are round blebs or elongate seams of microspar (Fig. 3d). Internal brecciation is common.	Ra	3c,d
carbonate mudstone	Planar laminated (sub-mm scale) calcimudstone or dolomudstone. As dolomudstone, the facies is resistant and tan-weathering. As calcimudstone, it is fissile or flaggy and dark grey.	Ra, Gf	3e,f
sandstone	Bedded or channelized sandstone and conglomerate. Dominant lithology is moderately well-sorted, well-cemented fine quartz sandstone. Minor lithologies include very coarse angular lithic sandstone and pebble conglomerate.	CF	6a
interbedded siliciclastics	Interbedded silt, shale and either nodular dolostone or indurated very fine quartz sandstone with low-angle (hummocky) cross-stratification. Silt is generally maroon; grey shale is more resistant than subcropping black shale, common in these sections.	Ra	6b
siltstone	Maroon to grey-green weathering siltstone, commonly poorly laminated to massive.	Ra, CF	6c
shale	Black shale, often present as subcrop.	Ra, CF	6d

Table 2. *Coordinates for the base and top of the stratigraphic sections in Figures 1 and 2.*

Section	Base		Top	
	Latitude	Longitude	Latitude	Longitude
G2447	64.8024	-139.7402	64.7988	-139.7704
CS2418	64.7988	-139.7704	64.7939	-139.7861
CS2202	64.7898	-139.7398	64.7852	-139.7556
CS2201	64.7841	-139.7011	64.7782	-139.7017
CS2309	64.7486	-139.5730	64.7464	-139.5725
CS2312	64.7435	-139.5662	64.7425	-139.5646
G2433	64.7317	-139.1925	64.7284	-139.1847
CS2414	64.7284	-139.1847	64.7246	-139.1792
G2442	64.7305	-139.1768	64.7278	-139.1785
CS2410	64.7294	-139.1229	64.7266	-139.1204
CS2411	64.7266	-139.1204	64.7246	-139.1187

interval of weathered black (organic-rich) shale. This is followed by laminated microbialite forming small domes, and microspar-void dolomudstone.

The microspar-void dolomudstone interval appears to thin to the west from the base (Fig. 7) and is adjacent to maroon-weathering siltstone. Some high-angle, dip-slip fault planes were observed in the siltstone of G2442. The first shale-to-carbonate cycle in the overlying Reefal assemblage is laterally continuous between the two ridges.

Section G2433/CS2414

A more complete section of the Fifteenmile Group is preserved on a ridge 2.5 km west of CS2410/11 and 200 m west of G2442 (64.7284°N, 139.1847°W; Figs. 1b and 2, Table 2). The Gibben formation in this section unconformably overlies flaggy yellow dolostone of the Gillespie Lake Formation (Wernecke Supergroup). The Gibben formation lithology alternates between yellow and grey-laminated dolostone including irregular brown chert, and well-sorted oolitic grainstone. The coarse, poorly sorted grainstone defining the upper contact of the Gibben formation is overlain by siltstone, which is the dominant lithology throughout the Chandindu Formation, punctuated by intervals of sandstone or conglomerate that are 1 to 3 m thick. The sandstone is generally thinly parallel-bedded, fine-grained quartz sandstone, whereas the conglomerate is a quartz-pebble conglomerate with a muddy matrix. Sand content decreases up-section.

The Reefal assemblage begins as organic-rich, black shale subcrop. The first 65 m of the section has four shale-to-carbonate cycles, which include some or all of the following facies (but consistently in this order): black shale; dolomudstone with abundant molar-tooth structure; faintly laminated microbial doloboundstone; and microspar-void dolomudstone with internal brecciation and small, elongate microspar seams but no molar-tooth structure. The microbial doloboundstone at 26 m includes outcrop faces with unusually good preservation of branching stromatolites.

These cycles are capped by another black shale interval. This is overlain by a 9 m-thick debrite bed, comprising tabular, angular clasts (1–40 cm length) of parallel-laminated dolomudstone in a dolomudstone matrix. The succeeding layer of microspar-void dolomudstone has regularly spaced (every ~8 cm) interbeds containing spherical chert (1–3 mm in diameter), which we interpret as silicified coated grains, and grades into unlaminated microbial doloboundstone including localized crinkly lamination and internal breccia.

The last outcrop of dolomudstone before the thick interval of microbial doloboundstone includes molar-tooth structure and is extensively recrystallized, in places resembling zebra dolomitization. The thick

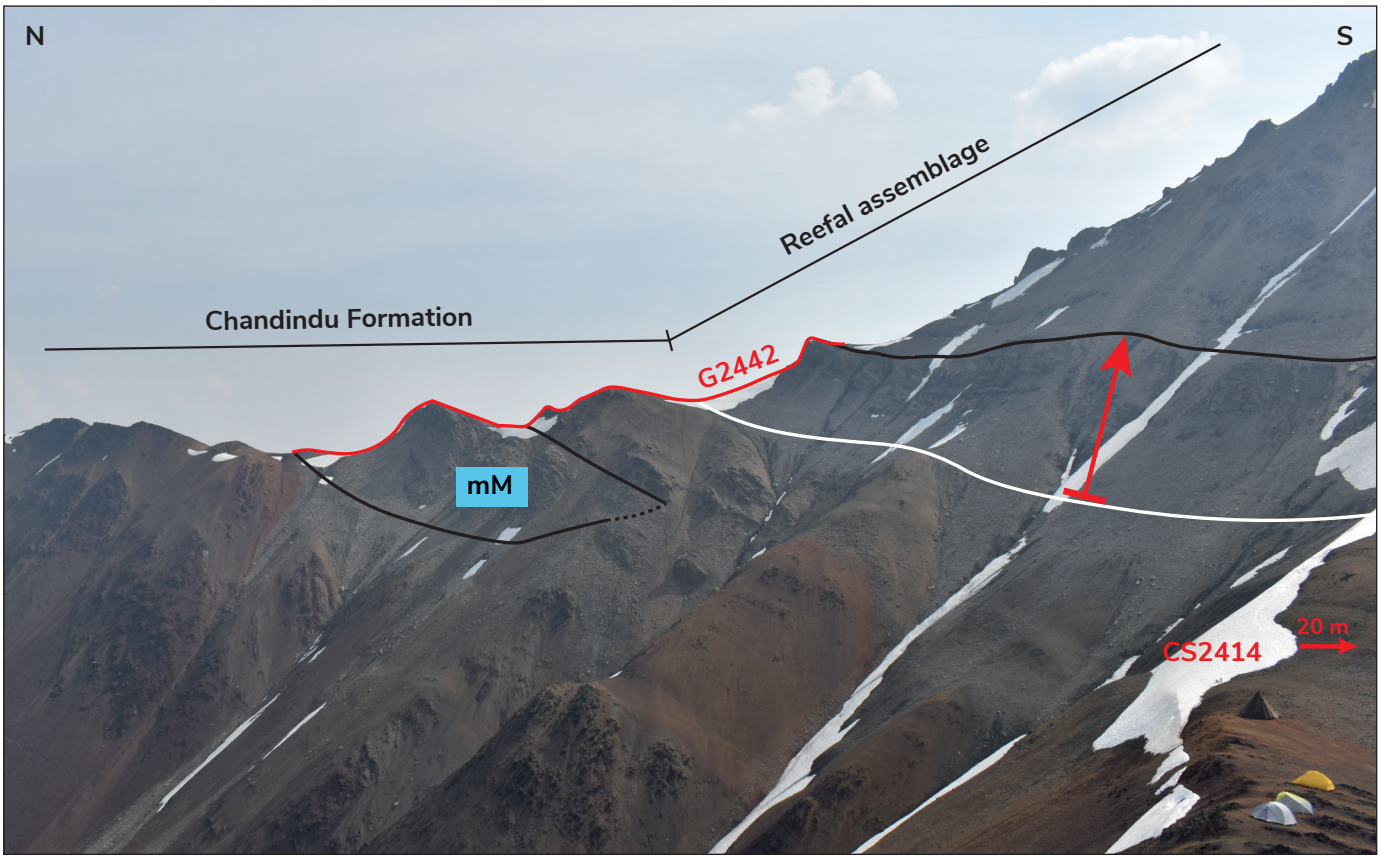

Figure 7. *Annotated photo of stratigraphic section G2442. An interval of microspar-void dolomudstone (mM) we assign to the Chandindu Formation thins to the west. The first shale-to-carbonate cycle (red arrow; black line is top of cycle) of the Reefal assemblage is laterally continuous across the ridge and is also measured by stratigraphic section CS2414. Tents, for scale, are ~2.5 m across.*

section of microbial doloboundstone begins at 130 m, and is generally massive with local preservation of cavities within the microbial framework, which are defined by curved protruding edges of the microbialite and filled with internal sediment (Fig. 5b). No clear lamination or growth direction is apparent. At the top of the exposure, the unlaminated microbialite forms domal bioherms ~1 m in diameter.

The thick microbialite interval is overlain by black shale interbedded with dark grey dolomudstone dominated by tabular internal breccia, which commonly forms decimetre-scale buckled folds reminiscent of tepee structures. This is followed by an interval of crinkly laminated, tan-weathering, recessive laminated microbialite doloboundstone. The rest of the section consists of mixed siliciclastic and fine-grained carbonate sedimentary rocks, including parallel-laminated dolomudstone containing shale partings and thin lenses of fine sand, dolomudstone with buckled tabular breccia, and interbedded black shale and dolomudstone with extensive molar-tooth structure and internal brecciation. The Reefal assemblage is capped by a distinctive 15 m-thick interval of interbedded maroon silt, shale, and very fine sandstone displaying hummocky cross-stratification (HCS), forming parasequences 1 to 2 m thick. At the base of the parasequences, very fine calcitic sandstone occurs in clear hummocks and swales within shale and silt, then sandstone layers become thicker and more laterally continuous toward the top of the parasequence. After an interval of recessive cover, the Craggy dolostone appears as a prominent outcrop of highly silicified, parallel-laminated, fine grainstone containing rare, low-angle cross-lamination and a tabular-clast breccia at its base.

Northern exposure belt (east to west)

Section CS2309/12

The exposure at this locality (64.7486°N, 139.5730°W; Figs. 1b and 2, Table 2) commences with discontinuous,

faintly laminated, microbial doloboundstone. The texture of these rocks is not clearly visible on outcrop faces, but irregular orange-weathering dolomite microspar cavities define discontinuous laminations that are predominantly parallel to regional bedding but are locally variable. At 91 m, the outcrop becomes laterally continuous across the ridge, and in the upper 5 m of doloboundstone, sheet cavities are lined by orange-weathering dolomite microspar. These microbialites are overlain by blue and red-weathering dolomudstones and calcimudstones, which can feature molar-tooth structure and round microspar blebs.

The next exposure is unlaminated microbialite, which at the base is highly silicified, accentuating vertical dendritic growth patterns similar to the dendritic face of CS2410/11 (at stratigraphic height of 170 m; Fig. 5a). Locally, this texture appears within metre-scale bioherms, where unlaminated microbialite is capped by silicified laminated stromatolites (Fig. 4f). Above the lowermost 5 m of the outcrop, the texture of the rock transitions to massive unlaminated microbialite doloboundstone. Lenses of debrites with silicified clasts were also found approximately 25 m along strike from the microbialite doloboundstone.

Above the unlaminated microbialite is a dip-slope of recessive shale, from which multiple isolated outcrops of faintly laminated microbialite emerge (Mb_L; Fig. 8a). The textures in these isolated build-ups are faintly laminated, in places exhibiting similarities to the columnar texture of the limestone in CS2418. Lamination orientation varies across the build-ups, and the south-facing edges have lamination approximately parallel to regional bedding, whereas the north-facing edges have lamination that is very steep relative to regional bedding (Fig. 8b).

Section CS2309 ends at the top of the microbialite outcrop, and section CS2312 (Fig. 1b) begins approximately 30 m stratigraphically above, and 200 m laterally, from the top of CS2309. This section commences with an outcrop of organic-rich shale overlain by unlaminated, massive, light-coloured dolomite we interpret as microbialite doloboundstone. Matrix-supported breccias of white, very fine carbonate also occur within these exposures, one of which has a sharp steep contact between breccia and microbialite, implying the clasts are derived from the microbialite. Above a thin interval of cover is a very coarse, highly silicified debrite, which we interpret as the base of the Craggy dolostone. Other debrite beds within the Craggy dolostone comprise tabular, silicified clasts, and local erosive bases.

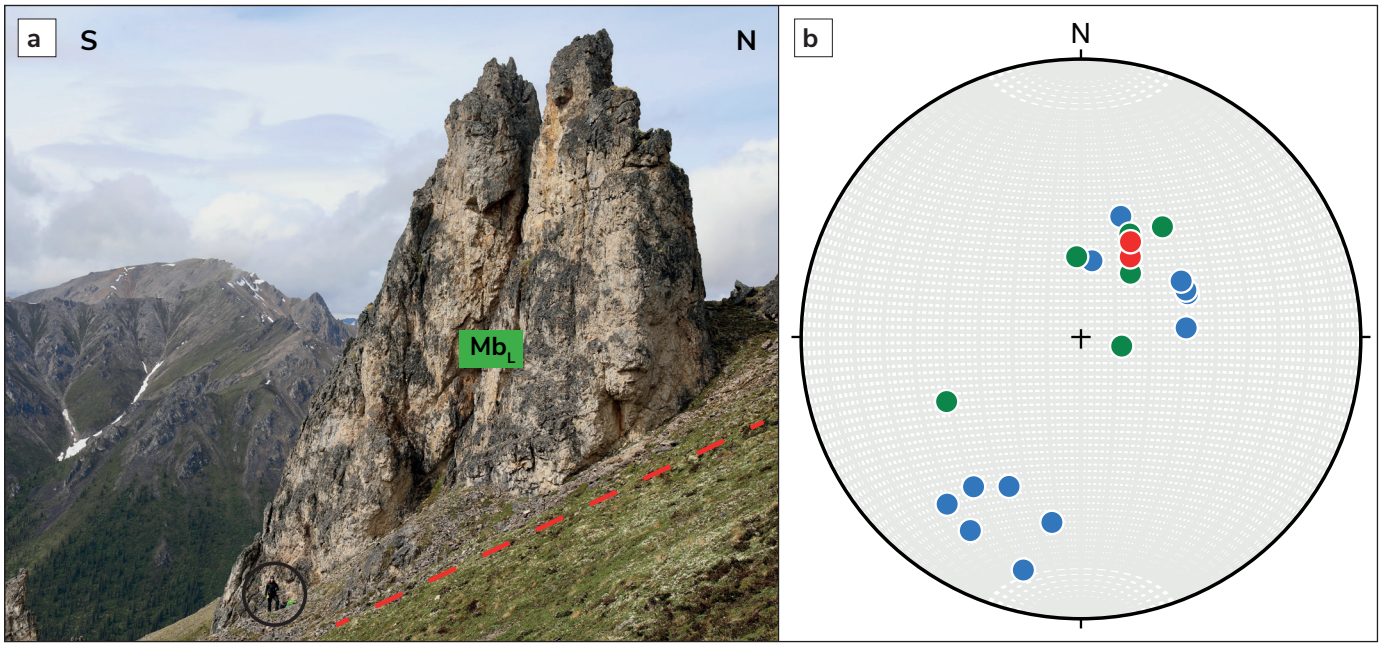

Figure 8. (a) *Annotated photo of isolated build-ups of laminated microbialite doloboundstone (Mb_L) emerging from a dip-slope (red dashed line). Location is adjacent to the top of stratigraphic section CS2309. Person for scale, circled in black.* ***(b)*** *Stereonet displaying poles to regional bedding (red), microbial lamination from isolated build-ups (blue) and microbial lamination from stratigraphic section CS2309 (green).*

Section CS2201

Section CS2201 (64.7842°N, 139.7010°W; Figs. 1b and 2, Table 2) begins with an abrupt transition from the red-weathering siltstone of the Chandindu Formation to organic-rich shale of the basal Reefal assemblage. The lowermost exposure of laminated microbialite at CS2201 is distinct from other sections, comprising localized partings of shale and internal brecciation between domal stromatolites with simple lamination and no cements or cavities. This interval is capped by a bed of siltstone and is followed by three successive beds of laminated microbialite with faint microspar-filled fenestrae, interbedded with black shale.

In the next 140 m of section, shale intervals alternate with various lithofacies of dolostone. In the lower part of this interval, the carbonate layers are highly brecciated molar-tooth dolomudstone that are significantly darker than the preceding microbialite. Up-section, the dolostone layers are faintly laminated tan-weathering microbialite doloboundstone, carbonate mudstone, and massive doloboundstone with no discernable features.

The uppermost 56 m of section CS2201 mostly comprises red shale to siltstone with thinly bedded, very fine grained quartz sandstone and orange dolostone, which become more common as interlayers up-section. This exposure is capped by laminated microbialite doloboundstone with metre-scale bioherms.

Section CS2202/G2235

The Chandindu Formation in this section (2.5 km west-northwest of section C2201: 64.7898°N, 139.7398°W; Figs. 1b and 2, Table 2) is dominated by siltstone, with beds of thinly laminated orange-weathering dolostone and coarse-grained quartz sandstone, which is typically laterally discontinuous. A transition from red-weathering mudstone to black shale marks the contact with the overlying Reefal assemblage. Four shale to microspar-void dolomudstone cycles follow, and contain molar-tooth structures in the upper 2–3 m of dolomudstone outcrop. The final cycle has microspar-void calcimudstone, rather than dolomudstone. This is followed by three intervals of faintly laminated microbialite doloboundstone, punctuated by shale and siltstone.

Section G2447/CS2418

In this section (1.6 km northwest of section CS2202: 64.8023°N, 139.7402°W; Figs. 1b and 2, Table 2), the Gibben formation overlies the yellow, flaggy dolomitic siltstone of the Gillespie Lake Group. The Gibben formation comprises medium-bedded, wavy laminated, grey-blue dolomudstone, with rare scour surfaces in the lower half of the section. The contact with the overlying Chandindu Formation begins with red-weathering shale and fine-grained quartz sandstone with polygonal (desiccation) cracks. The dominant lithology in the remaining section of Chandindu Formation is shaley siltstone, with abundant lenses of mostly fine, well-rounded quartz sandstone, and rare examples of dolomitic cement and HCS. By contrast, the more laterally continuous sandstone beds comprise angular, coarse-grained lithic sandstones. Microbialites and other carbonates are more abundant in this section than in sections farther east. The microbialites are dominated by unlaminated facies, with distinctive white to light grey cements in some beds highlighting the clotted texture. Microbialites variably form discontinuous metre-scale thick beds, commonly interbedded with shale, or low-relief metre-scale mounds.

The top of the Chandindu Formation is a well-cemented sandstone: a 3-m interval of quartz wacke with a distinct 10-cm bed of angular, very coarse lithic sandstone. Black shale dominates the first 90 m of the Reefal assemblage. Above the black shale interval, three cycles of calcimudstone contain extensive molar-tooth structure, grading into bedded organic-rich planar laminated calcimudstone. Above are six cycles with a reverse gradation of facies: shale, to fissile planar-laminated calcimudstone, to organic-rich wavy bedded calcimudstone, to thickly bedded calcimudstone with extensive molar-tooth structure.

The following 12 m section of limestone microbialite is exceptionally well preserved compared to the dolomite microbialite boundstone in other sections. It displays primary microbial textures, including differentiation between dense, locally columnar, clotted microbial framework, and cavities filled with internal sediment (Fig. 5c, d). Cavities are defined by protrusions of the microbialite, and in some cases, partial fill defines geopetal structures in which two generations of carbonate cement can be discerned (Fig. 5c). These geopetal structures are only seen in the centre of the outcrop. Within 5 m of the base and top, cavities are completely filled by internal sediment, and in the uppermost and lowermost 2 m of the exposure, the texture is obscured, transitioning into coarse mottling between grey and orange-weathering dolomite.

Above the limestone microbialite, alternating shale and silt are interbedded with 2–10 cm beds of well-indurated, very fine grained quartz sandstone with

low-angle cross stratification and nodular dolostone. Three subsequent, laterally discontinuous, outcrops of microbialite doloboundstone, separated by molar-tooth dolomudstone and black shale subcrop, have localized extensive silicification. Some faces with limited weathering reveal cavities partially filled with internal sediment. The uppermost microbialite doloboundstone weathers orange, and some cavities have a flat base and digitate roof (i.e., 'stromatactis' sensu, Aubrecht, 2011). Overlying shales are interbedded with nodular dolomite and indurated, very fine grained, HCS quartz sandstone.

The substantial unlaminated microbialite doloboundstone buildup in this section manifests predominantly as massive dolomite, with no visible cavities. Less weathered outcrop faces and blocks in float reveal faint cavities similar to the laterally discontinuous blocks and exceptionally preserved limestone microbialite below. No significant change in texture occurs up-section. The interval above the reef buildup is covered by vegetation, but laterally, the reefal buildup is draped by black shale (Fig. 9).

Above the covered, black shale interval is a succession of interbedded shale, silt, indurated very fine grained quartz sandstone, and planar-laminated limestone. It is overlain by tan-weathering laminated dolomite with extensive, buckled tabular internal breccia, and tepee structures. After 52 m, a prominent outcrop of recrystallized parallel-laminated grainstone defines the base of the Craggy dolostone.

Discussion

Facies associations

Both types of microbialite doloboundstone form extensive, laterally discontinuous outcrops, at times adjacent to shale (Fig. 9b). Certain sections also include shale-adjacent, discontinuous outcrops of microspar-void dolomudstone facies (e.g., Fig. 7). We therefore define the relief-forming reef core by the lithofacies assemblage of laminated microbialite doloboundstone, unlaminated microbialite doloboundstone and microspar-void dolomudstone. The facies adjacent to the reef core may be preliminarily split into two facies associations. The first is an association of carbonate mudstone, interbedded siliciclastics and laterally continuous beds of laminated microbialite (e.g., 244–364 m of CS2414, 179–205 m and 509–562 m of CS2418; Fig. 2). Given the presence of tepees, buckled internal breccia, low-relief stromatolites and HCS, we consider this facies association to be deposited in intertidal to supratidal water depth with periodic restriction, and therefore represents a back-reef lagoon on the proximal side of the reef core. By contrast, we consider the association of molar-tooth-dominated dolomudstone, debrite and shale to reflect deposition on a distally steepened ramp, and thick intervals of shale correspond to basinal deposition below storm-weather wave base.

Record of reef development

The sections spanning the Reefal assemblage demonstrate an overall up-section increase in the proportion of reef core lithofacies, particularly unlaminated microbialite doloboundstone. Although there is substantial variability across the inlier, the general trend is a transition from thick successions of shale with intervening microspar-void dolomudstone, to isolated outcrops of microbialite doloboundstone, to laterally continuous exposures of (generally unlaminated) microbialite doloboundstone up to 115 m thick. This transition is particularly apparent in the westernmost sections of both exposure belts in the Coal Creek inlier (CS2414 and CS2418; Fig. 1b). In the easternmost section of the northern belt (CS2309/12), patchy laminated microbialite precedes the onset of more substantial coverage.

We suggest that this transition is due to an overall shallowing and progradation of reefs as the basin filled, as inferred by Macdonald et al. (2012). In isolation, the increasing abundance of unlaminated microbialite is a poor depth indicator, given that Precambrian unlaminated microbialites have been inferred to develop in variable water depths and settings, including the deep slope and basin floor (Little Dal Group; Turner et al., 1997; Batten et al., 2004), lower-subtidal settings (Wumishan Formation; Tang et al., 2013), and near-vertical deep escarpments (Balcanoona Formation; Wallace et al., 2015). However, the increase in substantial unlaminated microbialite up-section is also accompanied by a decrease in the abundance of shale, as well as the appearance of a) interbedded siliciclastic facies with nodular limestone beds and fine HCS sandstone; and b) dolomudstone with tepee structures and buckled tabular breccias. Hummocky cross-stratification is characteristic of deposition between fair and storm-weather wave base (Dumas and Arnott, 2006), whereas tepees and buckled tabular breccia are characteristic of deposition in an intertidal to supratidal environment, where evaporation induces fluid escape and carbonate cementation (Kendall and Warren, 1987). Therefore, both facies represent a much

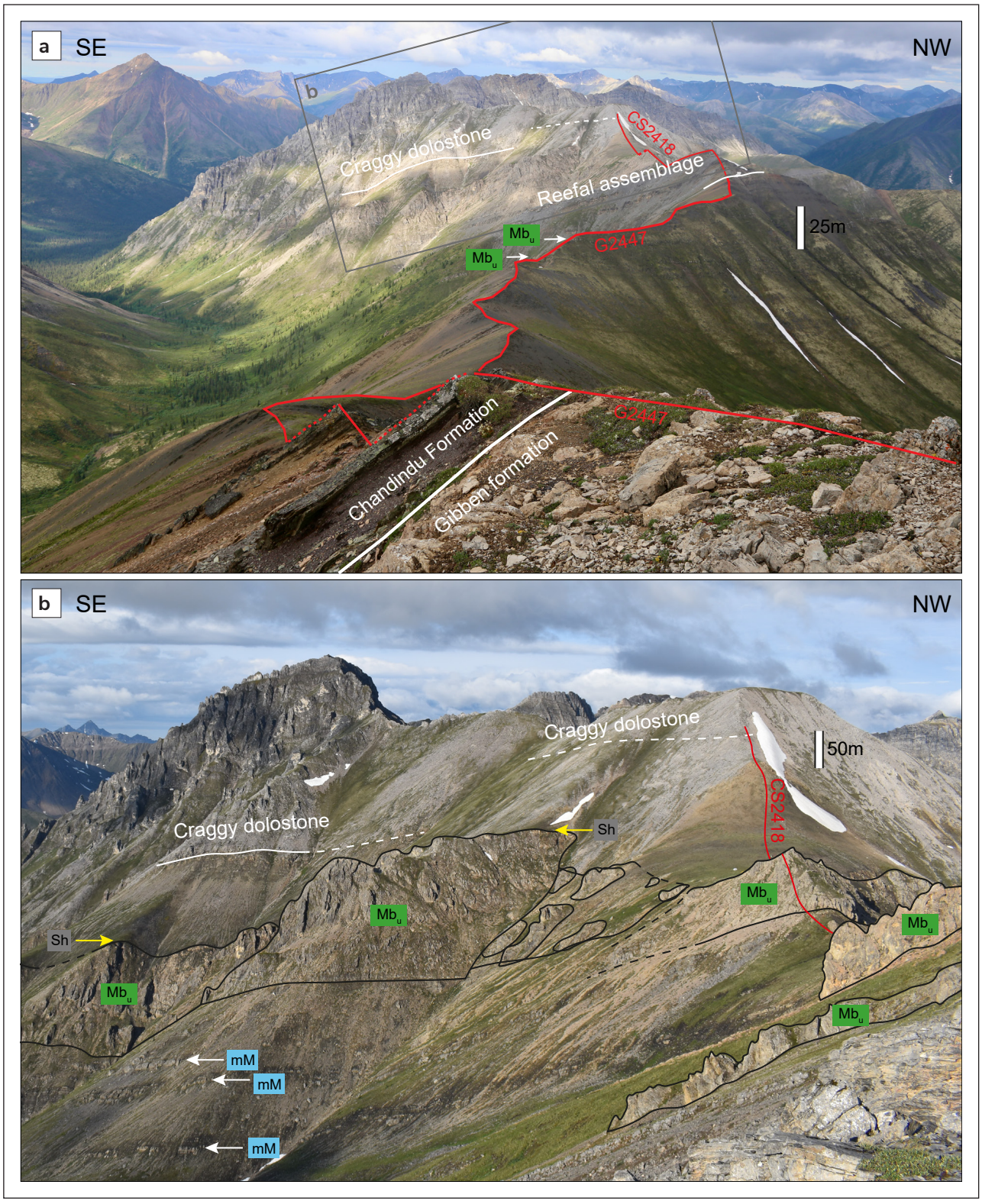

Figure 9. (a) *Annotated photo of stratigraphic section G2447. White arrows denote outcrops of unlaminated (clotted) microbialite (Mb_u).* ***(b)*** *Inset of (a); annotated photo of CS2418. Black outlines denote reefal outcrops of unlaminated microbialite, and yellow arrows denote the abrupt contact with black shale (Sh) above the southeastern outcrop. White arrows denote exposures of microspar-void dolomudstone (mM) capping shale-to-carbonate cycles. Scale varies with perspective; in both subplots, scale bars are applicable to their relevant place in the section.*

shallower depositional setting than the organic-rich shale characteristic of most of the Reefal assemblage. The interbedded siliciclastic facies is a common feature in the uppermost part of the Reefal assemblage (sections CS2418, CS2201 and CS2414), suggesting that by this point, shallow environments extended across the basin and terrigenous input may have increased. Furthermore, this shallowing-up sequence is followed conformably by the onset of the Craggy dolostone carbonate platform.

Within this context of an overall progradational succession, we identified regular, smaller-scale, shale-to-carbonate cycles in some sections of the Reefal assemblage. We interpret these as higher order transgressive-regressive cycles (Fig. 2), reflecting some combination of shallowing and increased carbonate saturation, possibly related to basin restriction. Regression is represented by a common motif of shale followed by molar-tooth carbonate mudstone. This motif varies across the basin; for example, section CS2418 also has an organic-rich calcimudstone facies between shale and molar-tooth calcimudstone. In section CS2414, the shale and molar-tooth dolomudstone is succeeded by faintly laminated microbialite doloboundstone and microspar-void dolomudstone with blebs and seams rather than molar-tooth structure. These latter facies may represent a lowstand system tract during which the basin was restricted. The generally sharp contacts with black shale atop each cycle are interpreted to record flooding with minimal to no transgressive systems tract being preserved.

The pattern of shale-to-carbonate cycles followed by thick, laterally extensive, microbialite is not seen in stratigraphic section CS2410/11. Here, reef core lithofacies begin lower in the section, and non-microbial facies are rare above this level. We interpret this difference to reflect a proximal setting closer to the reef core. As a result, high-order shale-to-carbonate cycles are absent, though changes in base level may correlate with shifts in the dominant microbialite morphology from laminated to unlaminated. At present, this remains a hypothesis, as our preliminary study cannot conclusively assign a depth control on microbialite morphology.

Significance of microbialite textures

The unlaminated microbialite calciboundstone in CS2418 (stratigraphic height 168 m) is exceptionally well-preserved (Fig. 5c, d). In four of our seven sections, we identified comparable features in rare preservation windows in otherwise massive and featureless dolostone. Although neither the internal structure of the microbialite nor different cement generations can be discerned in the field, preservational windows display cavities defined by clotted protrusions of microbialite, and columnar features and internal sediment (Fig. 5b) reveal their similar morphology to the calciboundstone in CS2418. Therefore, given the spectrum of unlaminated microbialite features, from featureless (Fig. 4d) to clotted, columnar and cavity-dense (Fig. 5c, d), we suggest that all the 'unlaminated microbialite doloboundstone' of the Reefal assemblage was originally framework-building, clotted microbialite similar to the calciboundstone in CS2418. The primary features of this microbialite are variably obscured by a variety of late-stage recrystallization and poor outcrop.

There are notable similarities and differences between the reefal textures of the Reefal assemblage and the deep-water reefs of the lower Little Dal Group (Stone Knife and Silverberry formations), which is thought to correlate to the Fifteenmile Group (Thomson et al., 2015a, b). The Little Dal reefs are also constructed by a mixture of laminated ('lamelliform') and unlaminated ('dendritic/clotted') microbialite textures (Turner et al., 1997). In addition, the shape of cavities in well-preserved calciboundstone and doloboundstone in the Reefal assemblage is very similar to the shape of cavities in the Little Dal clotted microbialite (Fig. 18.15b in James and Jones, 2015; Fig. 2f, g in Turner, 2021). However, the two reef systems differ in their scale and their depositional environment. The unlaminated microbialite reefs of the Little Dal had up to 100 m of topographic relief above a deep slope (Turner et al., 1997). By contrast, Reefal assemblage reefs formed in proximal environments (Macdonald et al., 2012). There is evidence that Reefal assemblage reefs formed on topographic highs, given the talus and olistoliths in basinal settings (Macdonald et al., 2012), and here we provide evidence that the reefs themselves were relief-forming, given the change in bedding orientation associated with isolated reef build-ups (Fig. 8) and the onlap of shale onto large reef exposures (e.g., Fig. 9b). However, we find no clear evidence for significant, continuous escarpments, or paleotopography on the scale of the Little Dal (up to 100 m). Nevertheless, the shale-to-carbonate repetitions in the basin, as well as the presence of talus and olistoliths (Macdonald et al., 2012), demonstrate that the Reefal assemblage was a long-lived, basin-scale carbonate factory.

Lateral variability in the Chandindu Formation

Our findings support previous lithological studies of the Chandindu Formation that identified siltstone and minor outcrops of sandstone, shale, dolomudstone, and a variable abundance of generally laterally discontinuous or mounded microbialite (Macdonald et al., 2012 Kunzmann et al., 2014). We note a bimodal distribution of coarse siliciclastic sediments: gritty, coarse, angular lithic sandstone, and fine, rounded, quartz sandstone with intermittent HCS. This likely reflects two distinct sediment sources, one more proximal and one more distal, and/or variably hyperpycnal and hypopycnal flow from delta channels (Zavala, 2020).

We note the higher proportion of carbonate in the western sections of the Chandindu Formation, and the clotted microbialite in the westernmost section (CS2418), which is similar to the unlaminated microbialite identified in the Reefal assemblage. We suggest that this demonstrates that marine conditions in the basin were already suitable for unlaminated reef development during deposition of the Chandindu Formation. However, as argued by Kunzmann et al. (2014), substantial reef development was generally prevented by the regular input of terrigenous detritus (e.g., through delta lobe switching), which may have been linked to ongoing extension and footwall uplift at this time (Macdonald et al., 2012). This interpretation also provides an explanation for the 50 m of microspar-void dolomudstone in the Chandindu Formation at section G2442. The continuity of the first shale-to-carbonate cycle of the Reefal assemblage (Fig. 7) suggests that the underlying microspar-void dolomudstone belongs to the Chandindu Formation and may be linked to proximal reef development. Furthermore, we placed the base of CS2410 above an approximately 100 m interval of microspar-void dolomudstone and unlaminated microbialite doloboundstone, assuming a thrusted contact. However, it is plausible that these lower reef facies belong to the Chandindu Formation, representing a successful reef in proximal settings.

The thicknesses of our complete measured sections of the Chandindu Formation (186 m for G2433, 540 m for G2447) differ significantly from one another and from the adjacent sections measured by Kunzmann et al. (2014). The discrepancy with previous studies may be partially explained by our recognition that the contact, as defined by an abrupt flooding and deposition of black shale, in places overlies interbedded coarse clastic rocks and microbial build-ups, which were originally assigned to the Reefal assemblage. The difference between our measured thicknesses and those of adjacent sections further emphasizes the pronounced basin topography that influenced deposition of the Fifteenmile Group.

Conclusion

Our findings support previous work (Macdonald et al., 2012) demonstrating that the Reefal assemblage is a basin-scale carbonate factory deposited in an overall progradational system in a basin with inherited extension-related topography. Suitable conditions for reef development began during deposition of the uppermost Chandindu Formation, although continuous siliciclastic input hampered substantial reef development. We have defined the contact between the Chandindu Formation and the Reefal assemblage as the distinct black shale flooding surface, which we interpret to strongly correlate across the basin, and above which siltstone is no longer the dominant lithology.

The Reefal assemblage is characterized by platformal microbialite, which alternates between laminated and unlaminated facies, and shale-to-carbonate cycles in the adjacent shale basin. The unlaminated facies of the reef was a framework-constructing microbialite, which is now primarily preserved as recrystallized massive dolostone, with primary growth features seen in rare preservation windows. These well-preserved microbialites have similar morphologies to the unlaminated reef systems in the Little Dal Group. Our work therefore provides additional evidence in favour of a transition in the nature of dominant reef-builders during the Tonian period.

Acknowledgments

We acknowledge that this project took place on the Traditional Territory of the Tr'ondëk Hwëch'in First Nation, and we are grateful for their permission to work on this land. The project was supported by the Polar Continental Shelf Program and NSERC Discovery and Northern Research Supplement grants to G. Halverson. Fireweed Helicopters provided safe and reliable transport to the field. We thank Lucy Webb, Maggie Whelan, Elizabeth Sullivan, Tyler Ambrose, Maddie Norman and Caroline Dee for their assistance in the field. We thank Rob Rainbird for his detailed review, which greatly improved this manuscript.

References

Aitken, J.D., 1967. Classification and environmental significance of cryptalgal limestones and dolomites, with illustrations from the Cambrian and Ordovician of southwestern Alberta. Journal of Sedimentary Research, vol. 37, p. 1163–1178. https://doi.org/10.1306/74D7185C-2B21-11D7-8648000102C1865D

Aubrecht, R., 2011. Stromatactis. *In*: Encyclopedia of Geobiology. Encyclopedia of Earth Sciences Series. J. Reitner and V. Thiel, (eds.), Springer Netherlands, Dordrecht, p. 847–850. https://doi.org/10.1007/978-1-4020-9212-1_226

Batten, K.L., Narbonne, G.M. and James, N.P., 2004. Paleoenvironments and growth of early Neoproterozoic calcimicrobial reefs: platformal Little Dal Group, northwestern Canada. Precambrian Research, vol. 133, p. 249–269. https://doi.org/10.1016/j.precamres.2004.05.003

Busch, J.F., Rooney, A.D., Meyer, E.E., Town, C.F., Moynihan, D.P. and Strauss, J.V., 2021. Late Neoproterozoic – early Paleozoic basin evolution in the Coal Creek inlier of Yukon, Canada: implications for the tectonic evolution of northwestern Laurentia. Canadian Journal of Earth Sciences, vol. 58, p. 355–377. https://doi.org/10.1139/cjes-2020-0132

Cohen, P.A., Strauss, J.V., Rooney, A.D., Sharma, M. and Tosca, N., 2017. Controlled hydroxyapatite biomineralization in an ~810 million-year-old unicellular eukaryote. Science Advances, vol. 3, issue 6, e1700095, https://www.science.org/doi/10.1126/sciadv.1700095

Colpron, M., Israel, S., Murphy, D., Pigage, L. and Moynihan, D., 2016. Yukon bedrock geology map. Yukon Geological Survey, Open File 2016-1, scale 1:1 000 000, map and legend.

Dumas, S. and Arnott, R.W.C., 2006. Origin of hummocky and swaley cross-stratification—The controlling influence of unidirectional current strength and aggradation rate. Geology, vol. 34, no. 12, p. 1073–1076. https://doi.org/10.1130/G22930A.1

Furlanetto, F., Thorkelson, D.J., Gibson, H.D., Marshall, D.D., Rainbird, R.H., Davis, W.J., Crowley, J.L. and Vervoort, J.D., 2013. Late Paleoproterozoic terrane accretion in northwestern Canada and the case for circum-Columbian orogenesis. Precambrian Research, vol. 224, p. 512–528. https://doi.org/10.1016/j.precamres.2012.10.010

Gibson, T.M., Faehnrich, K., Busch, J.F., McClelland, W.C., Schmitz, M.D. and Strauss, J.V., 2021. A detrital zircon test of large-scale terrane displacement along the Arctic margin of North America. Geology, vol. 49, no. 5, p. 545–550. https://doi.org/10.1130/G48336.1

Gibson, T.M., Kunzmann, M., Poirier, A., Schumann, D., Tosca, N.J. and Halverson, G.P., 2020. Geochemical signatures of transgressive shale intervals from the 811 Ma Fifteenmile Group in Yukon, Canada: Disentangling sedimentary redox cycling from weathering alteration. Geochimica et Cosmochimica Acta, vol. 280, p. 161–184. https://doi.org/10.1016/j.gca.2020.04.013

Green, L.H., 1972. Geology of Nash Creek, Larsen Creek, and Dawson map areas, Yukon Territory. Geological Survey of Canada, Memoir 364, 157 p. https://doi.org/10.4095/100697

Greenman, J.W., Rainbird, R.H. and Turner, E.C., 2020. High-resolution correlation between contrasting early Tonian carbonate successions in NW Canada highlights pronounced global carbon isotope variations. Precambrian Research, vol. 346, 105816. https://doi.org/10.1016/j.precamres.2020.105816

Greenman, J.W., Rooney, A.D., Patzke, M., Ielpi, A. and Halverson, G.P., 2021. Re-Os geochronology highlights widespread latest Mesoproterozoic (ca. 1090–1050 Ma) cratonic basin development on northern Laurentia. Geology, vol. 49, no. 7, p. 779–783. https://doi.org/10.1130/G48521.1

Grotzinger, J.P. and James, N.P., 2000. Precambrian carbonates: Evolution of understanding. *In*: Carbonate Sedimentation and Diagenesis in the Evolving Precambrian World, J.P. Grotzinger and N.P. James (eds.), SEPM Society for Sedimentary Geology, p. 320.

Halverson, G.P., Macdonald, F.A., Strauss, J.V., Smith, E.F., Cox, G.M. and Hubert-Théou, L., 2012. Updated definition and correlation of the lower Fifteenmile Group in the central and eastern Ogilvie Mountains. *In*: Yukon Exploration and Geology 2011, K.E. MacFarlane and P.J. Sack (eds.), Yukon Geological Survey, p. 75–90.

Halverson, G.P., Shen, C., Davies, J.H.F.L. and Wu, L., 2022. A Bayesian approach to inferring depositional ages applied to a Late Tonian reference section in Svalbard. Frontiers in Earth Science vol. 10. https://doi.org/10.3389/feart.2022.798739

James, N.P. and Jones, B., 2015. Origin of carbonate sedimentary rocks. John Wiley & Sons, West Sussex, UK, 454 p.

Kalkowsky, E., 1908. Oolith und Stromatolith im norddeutschen Buntsandstein. Zeitschrift der Deutschen Geologischen Gesellschaft vol. 60, p. 68–125. https://doi.org/10.1127/zdgg/60/1908/68

Kendall, C.G.St.C. and Warren, J., 1987. A review of the origin and setting of tepees and their associated fabrics. Sedimentology, vol. 34, p. 1007–1027. https://doi.org/10.1111/j.1365-3091.1987.tb00590.x

Kriscautzky, A., Kah, L.C. and Bartley, J.K., 2022. Molar-tooth structure as a window into the deposition and diagenesis of Precambrian carbonate. Annual Review of Earth and Planetary Sciences, vol. 50, p. 205–230. https://doi.org/10.1146/annurev-earth-031621-080804

Kunzmann, M., Halverson, G., Macdonald, F., Hodgskiss, M., Sansjofre, P., Schumann, D. and Rainbird, R., 2014. The early Neoproterozoic Chandindu Formation of the Fifteenmile Group in the Ogilvie Mountains, *In*: Yukon Exploration and Geology 2013, K.E. MacFarlane, M.G. Nordling and P.J. Sack, (eds.), Yukon Geological Survey, p. 93–107.

Macdonald, F.A. and Roots, C.F., 2010. Upper Fifteenmile Group in the Ogilvie Mountains and correlations of early Neoproterozoic strata in the northern Cordillera. *In*: Yukon Exploration and Geology 2009, K.E. MacFarlane, L.H. Weston and L.R. Blackburn (eds.), Yukon Geological Survey, p. 237–252.

Macdonald, F.A., Halverson, G., Strauss, J., Smith, E., Cox, G., Sperling, E. and Roots, C., 2012. Early Neoproterozoic Basin Formation in Yukon, Canada: Implications for the make-up and break-up of Rodinia. Geoscience Canada, vol. 39, no. 2, p. 77–100.

Macdonald, F.A., Schmitz, M.D., Crowley, J.L., Roots, C.F., Jones, D.S., Maloof, A.C., Strauss, J.V., Cohen, P.A., Johnston, D.T. and Schrag, D.P., 2010a. Calibrating the Cryogenian. Science, vol. 327, issue 5970, p. 1241–1243. https://doi.org/10.1126/science.1183325

Macdonald, F.A., Smith, E.F., Strauss, J.V., Cox, .M., Halverson, G.P. and Roots, C.F., 2010b. Neoproterozoic and early Paleozoic correlations in the western Ogilvie Mountains, Yukon. *In*: Yukon Exploration and Geology 2011, K.E. MacFarlane, L.H. Weston and C. Relf (eds.), Yukon Geological Survey, p. 161–182.

Medig, K.P.R., Turner, E.C., Thorkelson, D.J. and Rainbird, R.H., 2016. Rifting of Columbia to form a deep-water siliciclastic to carbonate succession: The Mesoproterozoic Pinguicula Group of northern Yukon, Canada. Precambrian Research, vol. 278, p.179–206. https://doi.org/10.1016/j.precamres.2016.03.021

Rainbird, R.H., Jefferson, C.W. and Young, G.M., 1996. The early Neoproterozoic sedimentary Succession B of northwestern Laurentia: Correlations and paleogeographic significance. GSA Bulletin vol. 108, no. 4, p. 454–470. https://doi.org/10.1130/0016-7606(1996)108<0454:TENSSB>2.3.CO;2

Rooney, A.D., Strauss, J.V., Brandon, A.D. and Macdonald, F.A., 2015. A Cryogenian chronology: Two long-lasting synchronous Neoproterozoic glaciations. Geology, vol. 43, no. 5, p. 459–462. https://doi.org/10.1130/G36511.1

Semikhatov, M.A., Gebelein, C.D., Cloud, P., Awramik, S.M. and Benmore, W.C., 1979. Stromatolite morphogenesis—progress and problems. Canadian Journal of Earth Sciences, vol. 16, no. 5, p. 992–1015. https://doi.org/10.1139/e79-088

Shapiro, R.S., 2000. A Comment on the systematic confusion of thrombolites. Palaios, vol. 15, no. 2, p. 166–169. https://doi.org/10.1669/0883-1351(2000)015<0166:ACOTSC>2.0.CO;2

Sperling, E.A., Halverson, G.P., Knoll, A.H., Macdonald, F.A. and Johnston, D.T., 2013. A basin redox transect at the dawn of animal life. Earth and Planetary Science Letters, vols. 371–372, p. 143–155. https://doi.org/10.1016/j.epsl.2013.04.003

Strauss, J.V., Roots, C.F., MacDonald, F.A., Halverson, G.P., Eyster, A. and Colpron, M., 2014. Geological map of the Coal Creek Inlier, Ogilvie Mountains (NTS 116B/10-15 and 116C/9, 16). Yukon Geological Survey, Open File 2014-15, scale 1:100 000.

Strauss, J.V., MacDonald, F.A., Halverson, G.P., Tosca, N.J., Schrag, D.P. and Knoll, A.H., 2015. Stratigraphic evolution of the Neoproterozoic Callison Lake Formation: Linking the break-up of Rodinia to the Islay carbon isotope excursion. American Journal of Science, vol. 315, p. 881–944. https://doi.org/10.2475/10.2015.01

Tang, D., Shi, X. and Jiang, G., 2013. Mesoproterozoic biogenic thrombolites from the North China platform. International Journal of Earth Sciences, vol. 102, p. 401–413. https://doi.org/10.1007/s00531-012-0817-9

Thompson, R.I. and Roots, C.F., 1982. Ogilvie Mountains project, Yukon; Part A: a new regional mapping program. Geological Survey of Canada, Paper 82-1A, p. 403–411 https://doi.org/10.4095/111324

Thompson, R.I., Roots, C.F. and Mustard, P.S., 1994. Geology of Dawson map area (116B,C) (northeast of Tintina Trench). Geological Survey of Canada, Open File, 2849. https://doi.org/10.4095/194830

Thomson, D., Rainbird, R.H. and Krapez, B., 2015a. Sequence and tectonostratigraphy of the Neoproterozoic (Tonian-Cryogenian) Amundsen Basin prior to supercontinent (Rodinia) breakup. Precambrian Research, vol. 263, p. 246–259. https://doi.org/10.1016/j.precamres.2015.03.001

Thomson, D., Rainbird, R.H., Planavsky, N., Lyons, T.W. and Bekker, A., 2015b. Chemostratigraphy of the Shaler Supergroup, Victoria Island, NW Canada: A record of ocean composition prior to the Cryogenian glaciations. Precambrian Research, vol. 263, p. 232–245. https://doi.org/10.1016/j.precamres.2015.02.007

Thorkelson, D.J., Abbott, J.G., Mortensen, J.K., Creaser, R.A., Villeneuve, M.E., McNicoll, V.J. and Layer, P.W., 2005. Early and middle Proterozoic evolution of Yukon, Canada. Canadian Journal of Earth Sciences, vol. 42, p. 1045–1071.

Turner, E.C., 2021. Possible poriferan body fossils in early Neoproterozoic microbial reefs. Nature, vol. 596, p. 87–91. https://doi.org/10.1038/s41586-021-03773-z

Turner, E.C., James, N.P. and Narbonne, G.M., 1997. Growth dynamics of Neoproterozoic calcimicrobial reefs, Mackenzie Mountains, Northwest Canada. Journal of Sedimentary Research, vol. 67, p. 437–450. https://doi.org/10.1306/D4268590-2B26-11D7-8648000102C1865D

Turner, E.C., James, N.P. and Narbonne, G.M., 2000. Taphonomic control on microstructure in early Neoproterozoic reefal stromatolites and thrombolites. Palaios, vol. 15, p. 87–111.

Turner, E.C., Narbonne, G.M. and James, N.P., 1993. Neoproterozoic reef microstructures from the Little Dal Group, northwestern Canada. Geology, vol. 21, no. 3, p. 259–262. https://doi.org/10.1130/0091-7613(1993)021<0259:NRMFTL>2.3.CO;2

Wallace, M.W., Hood, A.v.S., Woon, E.M.S., Giddings, J.A. and Fromhold, T.A., 2015. The Cryogenian Balcanoona reef complexes of the Northern Flinders Ranges: Implications for Neoproterozoic ocean chemistry. Palaeogeography, Palaeoclimatology, Palaeoecology, vol. 417, p. 320–336. https://doi.org/10.1016/j.palaeo.2014.09.028

Young, G.M., Jefferson, C.W., Delaney, G.D. and Yeo, G.M., 1979. Middle and late Proterozoic evolution of the northern Canadian Cordillera and Shield. Geology, vol. 7, no. 3, p. 125–128. https://doi.org/10.1130/0091-7613(1979)7<125:MALPEO>2.0.CO;2

Zavala, C., 2020. Hyperpycnal (over density) flows and deposits. Journal of Palaeogeography, vol. 9, article 17. https://doi.org/10.1186/s42501-020-00065-x